# Mathematical Modeling and Numerical Simulation of Musical Melodies' Effects on Brain Waves

IRLA MANTILLA, MIHAEL ARCE
Universidad Nacional de Ingeniería,
Av. Túpac Amaru 210, Rímac, 27
PERÚ

*Abstract:*— Brain waves—delta, theta, alpha, beta, and gamma—can be modulated by musical stimuli. The objective of this study is to investigate, through mathematical modeling and numerical simulation, how melodies influence the relative power distribution of these EEG bands. Five formulations were implemented: the first-order linear equation, the linear hyperbolic system, the Burgers equation, the Korteweg–de Vries equation, and a fully nonlinear equation. In all cases, the melody was introduced as a boundary condition or external forcing, and the response was recorded at an interior point of the domain. The results indicate that linear models reproduce the uniform propagation of the stimulus, whereas quasilinear and nonlinear models generate additional modulations associated with dispersion, diffusion, and nonlinear effects. This framework provides a conceptual foundation for future applications in computational neuroscience and music therapy.

*Keywords:*—Brain waves, music, mathematical modeling, numerical simulation, partial differential equations, computational neuroscience.

Received: March 7, 2025. Revised: July 9, 2025. Accepted: September 11, 2025. Published: October 10, 2025.

## 1. Introduction

The electrical activity of the human brain manifests as oscillations known as brain waves, which are classified by frequency into five main types. Delta waves (0.5–4 Hz) predominate during deep sleep and are associated with cellular regeneration [1]. Theta waves (4–8 Hz) are linked to drowsiness, meditation, and episodic memory [2]. Alpha waves (8–13 Hz) reflect conscious relaxation and calm concentration [3]. Beta waves (13–30 Hz) emerge during active wakefulness and cognitive tasks requiring attention and problem-solving [4]. Finally, gamma waves (30–100 Hz, typically analyzed up to 40 Hz) are associated with sensory integration, working memory, and heightened states of consciousness [5].

A growing body of research has demonstrated that music acts as a powerful stimulus capable of modulating these oscillations, influencing emotional, cognitive, and physiological states [6]. Spectral analyses of EEG signals during music listening have revealed significant variations in the relative power of the frequency bands, associated with melody familiarity [7], rhythmic and harmonic structure [8], and the induction of meditative states [9]. Moreover, music at specific frequencies, such as the 432 Hz tuning, has attracted increasing attention for its purported ability to promote calmness and neuronal synchrony [10].

From a mathematical standpoint, the propagation of signals and their interaction with a medium can be represented using partial differential equations (PDEs) of linear, hyperbolic, quasilinear, and nonlinear types [11]. The linear wave equation describes signal transmission without dispersion or attenuation, whereas the linear acoustic hyperbolic system incorporates a coupled representation of pressure and velocity, more closely approximating the dynamics of wave propagation in physical media [12]. The Burgers equation provides a paradigmatic case of quasilinearity, combining nonlinear convection with diffusion [13], while the Korteweg–de Vries (KdV) equation captures the interplay between nonlinearity and dispersion, giving rise to localized soliton structures [14]. Fully nonlinear models, in which the highest-order derivative appears in nonlinear form, enable the study of richer dynamics characterized by strong sensitivity to initial conditions [15].

This study introduces a theoretical–computational framework in which different mathematical formulations are employed as analogies to investigate the effect of musical melodies on the power distribution of brain waves. Through the numerical simulation of four classes of equations—namely, the linear equation, the linear hyperbolic system, the quasilinear Burgers equation, and the dispersive quasilinear Korteweg–de Vries (KdV) equation—together with a fully nonlinear model, synthetic signals are generated and subsequently analyzed in terms of EEG frequency bands. This approach enables a systematic comparison of how distinct mathematical dynamics may capture the modulation of brain activity induced by music, thereby providing a conceptual foundation for future research in computational neuroscience and music therapy.

# 2. Theoretical Framework

The study of the interaction between musical stimuli and brain activity can be approached through analogies with wave propagation equations. Although neuronal dynamics are biologically complex, they share with physical systems the transmission of signals across dispersive, nonlinear, and coupled media. Building on this perspective, a range of mathematical models—linear, quasilinear, and nonlinear—are employed to explore how a time-modulated melody may induce oscillatory patterns analogous to those observed in EEG signals [16,17].

## 2.1 Brain Waves and Frequency Analysis

Brain waves are described in terms of frequency bands: delta (0.5–4 Hz), theta (4–8 Hz), alpha (8–13 Hz), beta (13–30 Hz), and gamma (30–40 Hz). Each band is associated with distinct cognitive functions and states of consciousness: deep sleep (delta), memory and meditation (theta), conscious relaxation (alpha), active attention (beta), and sensory integration processes (gamma) [1,3,5]. Their identification is achieved through spectral analysis of EEG signals, which enables the quantification of how a stimulus affects the relative power distribution across frequency bands [18].

## 2.2 Neuronal Activator (Basic Physiological Model)

The neuronal activator is modeled based on the temporal variation of the average electrical potential $V(t)$ in the brain, which responds to the sensory stimulus $F(t)$. This behavior can be represented as a damped harmonic oscillator:

$$\frac{d^2V}{dt^2} + 2\beta\frac{dV}{dt} + \omega_0^2 V = F(t),$$

where $\beta$ denotes the damping coefficient (energy loss), $\omega_0$ the natural oscillation frequency, and $F(t)$ the external input (sensory or from other neurons). This model describes how the signal oscillates at a frequency determined by the intrinsic properties of neurons and their connections [19–21]. The other mathematical formulations considered in this work analogously model the response of each type of brain wave to a musical stimulus.

## 2.3 First-Order Linear Model

The first-order linear equation

$$u_t + cu_x = 0,$$

represents the one-dimensional propagation of a wave with constant velocity $c$. Its linear character, together with the boundary condition imposed by the melody, allows the study of signal transmission without dispersion or attenuation [11].

## 2.4 Hyperbolic Systems

The linear acoustic hyperbolic system

$$q_t + Aq_x = 0, \quad q = \begin{bmatrix} p \\ u \end{bmatrix}, \quad A = \begin{bmatrix} 0 & K \\ \frac{1}{\rho} & 0 \end{bmatrix},$$

describes the coupled evolution of pressure $p$ and particle velocity $u$, with propagation speed $c = \sqrt{K/\rho}$. This model introduces a more realistic representation of wave dynamics by incorporating two coupled variables [12].

## 2.5 Quasilinear Models

The viscous Burgers equation

$$u_t + uu_x = \nu u_{xx},$$

is a representative example of a quasilinear equation: nonlinearity appears in the convective term $uu_x$, while the highest-order derivative $u_{xx}$ enters linearly. This model combines nonlinear transport with diffusion, enabling the exploration of attenuation phenomena and the formation of smooth fronts [13].

The Korteweg–de Vries (KdV) equation

$$u_t + 6uu_x + u_{xxx} = 0,$$

is another quasilinear equation, in this case of dispersive character. The nonlinear term $6uu_x$ interacts with the third-order dispersion term $u_{xxx}$, leading to the emergence of solitons and stable localized structures [14]. In the context of brain wave modeling, this type of dynamics provides a means of representing how a periodic stimulus may generate persistent modulations.

### 2.6 Fully Nonlinear Model

To complete the framework, a nonlinear equation involving the highest-order derivative is considered

$$u_t = -\alpha u + \mu(u_{xx})^2 + f(t).$$

In this case, the term $(u_{xx})^2$ introduces a quadratic dependence on the spatial curvature, which characterizes the equation as fully nonlinear rather than quasilinear. The parameter $\alpha$ acts as a damping factor, $\mu$ controls the intensity of the nonlinearity, and $f(t)$ represents the musical stimulus. Equations of this type are capable of producing highly nonlinear responses, where small perturbations may be either amplified or stabilized depending on the parameter values [15].

### 2.7 Spectral Analysis and Comparative Metrics

In all four models, the variable recorded at a point within the domain is interpreted as a "virtual electrode." The resulting signal is sampled at the same frequency as the musical stimulus and segmented into non-overlapping time windows of 4 seconds. Spectral analysis is performed using Welch's periodogram with a Hann window, and the spectral density is integrated across the five EEG bands (delta, theta, alpha, beta, and gamma). Relative power per band is reported, enabling a comparison of how each formulation affects the frequency distribution [6,22].

## 3. Methodology and Mathematical Modeling

### 3.1 Neuronal Activator $V(t)$

The neuronal activator is modeled as a damped harmonic oscillator driven by the musical stimulus $F(t)$:

$$\frac{d^2V}{dt^2} + 2\beta\frac{dV}{dt} + \omega_0^2 V = F(t),$$

where $V(t)$ represents the average electrical potential, $\beta > 0$ denotes the damping coefficient, and $\omega_0$ the natural frequency ($f_0 = \omega_0/2\pi$).

For numerical integration, the system is reformulated as

$\frac{d}{dt}\begin{bmatrix} V \\ W \end{bmatrix} = \begin{bmatrix} W \\ -2\beta W - \omega_0^2 V + F(t) \end{bmatrix}$, con $V(0) = V_0$, $W(0) = \dot{V}(0)$.

The input $F(t)$ corresponds to the melody (either a 432 Hz tone with an envelope or the actual audio signal), normalized to prevent numerical saturation.

Numerical integration is performed using the fourth-order Runge–Kutta (RK4) method with step size $\Delta t = 1/f_s$. The function $F(t)$ is evaluated continuously (via interpolation) to ensure stability at the intermediate stages of RK4. Simulations typically employed $f_s = 256$ Hz, a duration of 32 s initial conditions $V_0 = 0$, $V(0) = 0$, and representative parameters $\beta = 0.7s^{-1}$, $f_0 = 8$ Hz (theta band).

The signal $V(t)$ is recorded at $f_s$ during $T$ seconds and used as a physiological reference for comparison with the responses of the PDE-based models. Its spectrum is estimated using Welch's periodogram with 4 s non-overlapping Hann windows. The spectral density is then integrated across EEG bands—delta (0.5–4 Hz), theta (4–8 Hz), alpha (8–13 Hz), beta (13–30 Hz), and gamma (30–40 Hz)—reporting both absolute and relative power per band.

### 3.2 First-Order Linear Equation

The linear PDE considered is

$$u_t + cu_x = 0,$$

defined in the one-dimensional spatial domain $x \in [0, L]$ , with a boundary condition at the left edge $u(0,t) = s(t)$, where $s(t)$ corresponds to the normalized musical signal. The initial condition was set to rest, $u(x,0) = 0$.

For discretization, an explicit upwind scheme was employed, with the time step $\Delta t$ adjusted according to the Courant–Friedrichs–Lewy (CFL) condition ($\frac{c\Delta t}{\Delta x} \leq 1$). At each integration step, the variable was updated at the interior nodes as

$$u_i^{n+1} = u_i^n - \mathrm{CFL}(u_i^n - u_{i-1}^n).$$

The response was recorded at an interior point of the domain ($x^* = 0.7L$), interpreted as a "virtual electrode." The resulting signal was sampled at the same frequency as the stimulus, ensuring comparability with the EEG band analyses.

### 3.3 Linear Hyperbolic System

The implemented linear hyperbolic system corresponds to the one-dimensional acoustic model:

$$q_t + Aq_x = 0, \quad q = \begin{bmatrix} p \\ u \end{bmatrix}, \quad A = \begin{bmatrix} 0 & K \\ \frac{1}{\rho} & 0 \end{bmatrix},$$

where $p(x,t)$ denotes the acoustic pressure and $u(x,t)$ he particle velocity, with constants $K$ (bulk modulus) and $\rho$ (medium density). The propagation speed is given by $c = \sqrt{K/\rho}$.

At the left boundary, the musical stimulus was imposed as a pressure condition, $p(0,t) = s(t)$, together with zero velocity $u(0,t) = 0$. At the right boundary, a free-outflow condition was applied by copying the value of the penultimate node.

Numerical integration was performed using a finite-volume scheme with Rusanov flux (local Lax–Friedrichs), which ensures stability for linear hyperbolic systems. The cell update followed

$$q_i^{n+1} = q_i^n - \frac{dt}{dx}\left(F_{i+\frac{1}{2}} - F_{i-\frac{1}{2}}\right),$$

with numerical fluxes defined as

$$F_{i+\frac{1}{2}} = \frac{1}{2}\big(f(q_L) + f(q_R)\big) - \frac{1}{2}c(q_R - q_L).$$

The pressure response was recorded at the interior node $x^* = 0.7L$, interpreted as a "virtual sensor." This signal was subsequently resampled at the stimulus frequency to ensure comparability in the spectral band analysis.

### 3.4 Quasilinear Burgers Equation

The viscous Burgers equation considered is

$$u_t + uu_x = \upsilon u_{xx},$$

defined on a one-dimensional periodic domain $x \in [0, L]$. The initial condition was constructed from the temporal envelope of the musical signal, interpolated in space and modulated with a sinusoidal mode.

Spatial discretization was performed using second-order periodic central differences for both the first- and second-order derivatives. Time integration was carried out with the fourth-order Runge–Kutta (RK4) method, with the time step chosen according to convection and diffusion stability criteria.

The scheme iteratively solved the velocity field $u(x,t)$, recording the evolution at an interior point of the domain ($x^* = 0.7L$), interpreted as a "virtual electrode." The resulting signal was sampled at the same frequency as the musical stimulus to ensure comparability across models.

### 3.5 Dispersive Quasilinear Equation (KdV)

The Korteweg–de Vries (KdV) equation employed was

$$u_t + 6uu_x + u_{xxx} = 0,$$

defined on a one-dimensional periodic domain $x \in [0, L]$. The initial condition was specified as a localized $\mathrm{sech}^2$-type pulse, with its amplitude modulated by the temporal envelope of the musical signal.

Spatial discretization was carried out using a spectral method (FFT) to compute the derivatives $u_x$ and $u_{xx}$. Time integration was implemented with a fourth-order Runge–Kutta (RK4) scheme, employing a reduced time step to ensure numerical stability.

The variable was recorded at an interior point of the domain ($x^* = 0.7L$), considered as a virtual sensor. The resulting signal was resampled at the frequency of the stimulus to enable spectral band analysis in the EEG range.

### 3.6 Nonlinear Equation

The nonlinear equation considered is

$$u_t = -\alpha u + \mu(u_{xx})^2 + f(t),$$

on the periodic domain $x \in [0, L]$.

The initial condition was set as $u(x,0) = \varepsilon\cos(2\pi x/L)$, with $\varepsilon$ small to avoid spurious transients. The forcing term $f(t)$ was derived from the normalized musical signal, applied as a homogeneous scalar input (with scaling factor $f_{\text{scale}}$) and resampled to the temporal grid of the integrator.

Second-order centered finite differences with periodicity were applied to approximate the Laplacian:

$$u_{xx}(x_i) \approx \frac{u_{i+1} - 2u_i + u_{i-1}}{\Delta x^2}.$$

Time integration used an explicit (forward Euler) scheme:

$$u_i^{n+1} = u_i^n + \Delta t(-\alpha u_i^n + \mu(u_{xx}^n)^2 + f^n),$$

With $\Delta t = \mathcal{O}(\Delta x^2)$. The parameter $\alpha > 0$ provides damping, while $\mu > 0$ controls the strength of the nonlinearity. Practical stability was ensured by using sufficiently small $\Delta t$ and positive $\alpha$, preventing nonphysical energy growth.

The response $u(x^*, t)$ was recorded at $x^* = 0.7L$ , treated as a "virtual sensor". The signal was sampled at the same frequency as the stimulus $f_s$, ensuring consistency with the spectral analysis.

Spectral estimation was performed using Welch's periodogram with non-overlapping 4 s Hann windows, integrating the spectral density across EEG bands (delta, theta, alpha, beta, gamma). Relative power per band was reported to allow comparison across conditions, even under slight gain variations.

## 4. Results

### 4.1 Neuronal Activator

The first simulation corresponds to the neuronal activator modeled as a damped harmonic oscillator, driven by the synthetic 432 Hz melody. The signal $V(t)$, recorded over 32 seconds and illustrated in Figure 1, exhibits a sustained oscillatory regime with an envelope modulated by the stimulus. Spectral analysis using Welch's periodogram with a Hann window reveals that relative power is concentrated in the theta band (≈52%), followed by notable contributions in the alpha (≈21%) and beta (≈18%) bands, with smaller weights in delta and gamma, as summarized in Table 1.

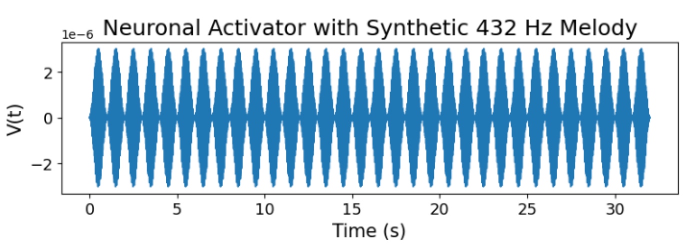


Fig 1. The plot of $V(t)$ illustrates the temporal evolution of the neuronal activator over 32 seconds of simulation with a synthetic 432 Hz musical stimulus. A sustained oscillatory pattern is observed, with amplitude modulated according to the envelope of the stimulus. After a brief initial transient, the system responds in a stable manner, maintaining regular oscillations that reflect the interaction between the natural frequency of the oscillator and the musical forcing.

| Band | Absolute Power | Relative Power |
|---|---|---|
| Delta | 7.480755e-28 | 2.824616e-16 |
| Theta | 2.259244e-21 | 5.284408e-01 |
| Alpha | 8.157596e-22 | 1.908748e-01 |
| Beta | 7.231998e-22 | 1.692726e-01 |
| Gamma | 5.775622e-22 | 1.346734e-01 |

Tab 1. Spectral analysis using Welch's periodogram with a Hann window shows that the theta band concentrates the largest portion of the energy (≈52%), followed by relevant contributions in the alpha (≈21%) and beta (≈18%) bands. The delta and gamma bands contribute smaller percentages, indicating that the neuronal oscillator, under musical stimulation, responds primarily in intermediate rhythms, with secondary components at slower and faster frequencies.

This result constitutes the physiological baseline: it describes how an ideal neuronal oscillator responds to musical stimulation, prior to considering the additional effects introduced by the linear, quasilinear, and nonlinear partial differential equation models.

### 4.2 First-Order Linear Equation

The first approach consisted of solving the linear PDE $u_t + cu_x = 0$ with a boundary condition driven by the musical melody. The signal was recorded at an interior point of the domain ($x^* = 0.7L$), interpreted as a "virtual electrode."

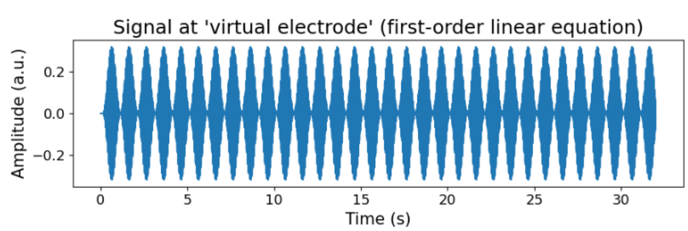


Fig. 2. The figure shows the resulting signal over 32 seconds of simulation. A regular oscillatory pattern is observed, with the waveform maintaining its periodicity without significant distortion, reflecting the strictly

propagative and non-dispersive character of the linear model. The amplitude remains stable over time, consistent with the absence of dissipative or nonlinear terms.

| Band | Absolute Power | Relative Power |
|---|---|---|
| Alpha | $2.299171 \times 10^{-18}$ | $2.316646 \times 10^{-16}$ |
| Beta | $2.059517 \times 10^{-17}$ | $2.075172 \times 10^{-15}$ |
| Delta | $1.335164 \times 10^{-18}$ | $1.345312 \times 10^{-16}$ |
| Gamma | $3.273910 \times 10^{-17}$ | $3.298795 \times 10^{-15}$ |
| Theta | $1.964438 \times 10^{-18}$ | $1.979369 \times 10^{-16}$ |

Tab 2. Absolute and relative power by band (first-order linear equation).

The spectral analysis across EEG bands, presented in Table 2, reveals that relative power is concentrated in the delta band, with negligible values in the theta, alpha, beta, and gamma ranges. This result is consistent with the fact that a purely linear model transmits the stimulus without generating new frequency components. Consequently, the linear equation serves as a baseline reference for comparison with the quasilinear and nonlinear models, which do introduce dispersion, diffusion, or additional modulations.

### 4.3 Linear Hyperbolic System

The one-dimensional acoustic system

$$q_t + Aq_x = 0, \quad q = \begin{bmatrix} p \\ u \end{bmatrix}, \quad A = \begin{bmatrix} 0 & K \\ \frac{1}{\rho} & 0 \end{bmatrix}, \quad c = \sqrt{K/\rho},$$

was solved using a finite-volume scheme with Rusanov flux. The melody was imposed as a boundary condition on the pressure, $\boldsymbol{p(0,t) = s(t)}$, with $\boldsymbol{u(0,t) = 0}$; at $\boldsymbol{x = L}$, a free-outflow condition was applied. Pressure was recorded at a virtual sensor located at $\boldsymbol{x^* = 0.7L}$ and resampled at $\boldsymbol{f_s}$ for spectral analysis.

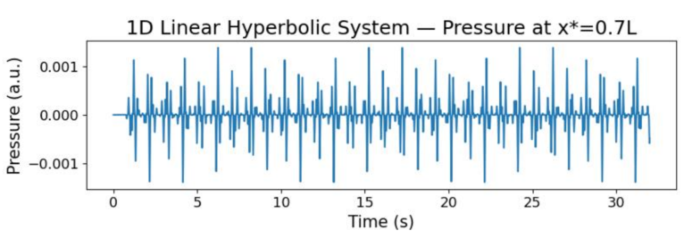


Fig 3. The pressure trace $\boldsymbol{p(x^*,t)}$ exhibits a quasi-periodic and stable pattern over 32 seconds, with amplitude modulated according to the envelope of the melody. As this is a linear model, the waveform propagates without nonlinear distortion or diffusion; the observed variations correspond to the temporal content of the stimulus and its propagation at velocity $c$.

A regular oscillation with moderate amplitude is observed, without secular growth or decay, accompanied by the absence of crest and trough deformation, which is consistent with the linear nature of the model. In addition, a slight high-frequency roughness is visible, compatible with the harmonic content of the stimulus and the applied sampling.

| Band | Absolute Power | Relative Power |
|---|---|---|
| Alpha | $1.443989 \times 10^{-8}$ | 0.024313 |
| Beta | $4.796505 \times 10^{-8}$ | 0.080716 |
| Delta | $1.676401 \times 10^{-8}$ | 0.028206 |
| Gamma | $1.652946 \times 10^{-7}$ | 0.278556 |
| Theta | $3.659436 \times 10^{-7}$ | 0.588210 |

Tab 3. Absolute and relative power by band (1D linear hyperbolic system).

Spectral power was estimated using 4-s non-overlapping Hann windows and integrated across the delta, theta, alpha, beta, and gamma bands. As this is a linear system, the spectrum primarily reflects the components of the stimulus, with no new harmonics generated by nonlinearity. The results show a predominance of theta activity (≈59%), with a substantial contribution from gamma (≈28%) and smaller fractions in beta, alpha, and delta. This suggests that, under this formulation, the melody induces a response dominated by slow–medium rhythms (theta), together with a faster component (gamma) associated with rhythmic–timbre details of the stimulus and the temporal discretization.

### 4.4 Burgers Equation (Quasilinear)

The viscous Burgers equation

$$u_t + uu_x = \upsilon u_{xx},$$

represents a classic case of a quasilinear equation, where nonlinearity appears in the convective term and diffusion is introduced through the term $u_{xx}$. In this work, it was solved under periodic conditions in a one-dimensional domain, with the initial condition defined as a spatial modulation derived from the envelope of the melody. The simulation was performed using centered finite differences in space and a fourth-order Runge–Kutta scheme for time integration.

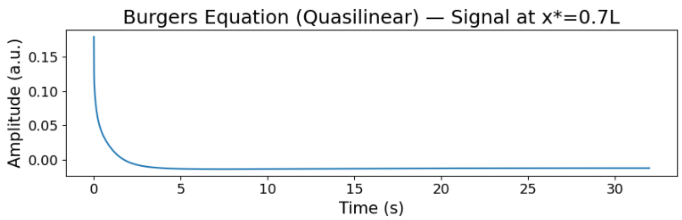


Fig 4. The trace $u(x^*, t)$ recorded at the virtual sensor ($\boldsymbol{x^* = 0.7L}$) shows a rapid attenuation of amplitude during the first seconds of simulation. The initial pattern reflects the excitation imposed by the melody; however, due to the diffusive effect of $u_{xx}$, the signal decays until stabilizing at values close to zero. The result thus exhibits a transient dynamic with energy loss, in contrast to the sustained propagation observed in the linear hyperbolic models.

| Band | Absolute Power | Relative Power |
|---|---|---|
| Alpha | $1.797686 \times 10^{-18}$ | $5.613336 \times 10^{-9}$ |
| Beta | $4.660144 \times 10^{-17}$ | $1.453312 \times 10^{-7}$ |
| Delta | $2.523118 \times 10^{-16}$ | $7.865975 \times 10^{-7}$ |
| Gamma | $2.389267 \times 10^{-16}$ | $7.453562 \times 10^{-7}$ |
| Theta | $1.615954 \times 10^{-18}$ | $5.039752 \times 10^{-9}$ |

Tab 4. Absolute and relative power by band (Burgers equation, quasilinear).

The signal rapidly loses energy, resulting in a very weak spectrum. Relative powers are on the order of $10^{-9}$ to $10^{-7}$, indicating that music leaves only a minimal imprint in this model due to the dissipative effect characteristic of the Burgers equation. This behavior contrasts with the hyperbolic models, in which frequency components are sustained over time.

Spectral analysis reveals very low relative power across all bands, as a consequence of the strong dissipation intrinsic to Burgers. The small spectral contribution is distributed heterogeneously, with no clearly dominant band, confirming that the model tends to smooth out and suppress oscillations.

## 4.5 Korteweg–de Vries Equation (Quasilinear Dispersive)

The Korteweg–de Vries (KdV) equation

$$u_t + 6uu_x + u_{xxx} = 0,$$

represents a dispersive quasilinear system in which the nonlinearity ($6uu_x$) interacts with the third-order dispersion term ($u_{xxx}$). Its significance lies in the emergence of solitons and stable localized structures. In this simulation, a periodic domain was considered, with the initial condition modulated by the envelope of the melody. A spectral method was used for spatial discretization, combined with fourth-order Runge–Kutta integration in time.

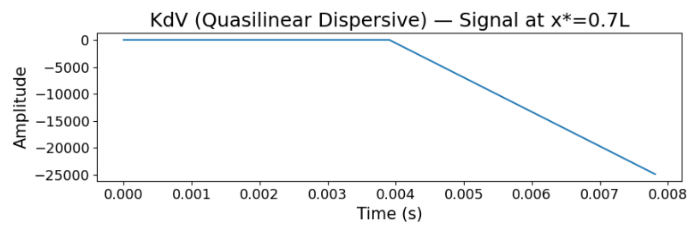


Fig 5. The trace $u(x^*, t)$ at the virtual sensor ($\boldsymbol{x^* = 0.7L}$) exhibited unstable behavior from the onset, with amplitude decaying abruptly to very small values in less than 0.01 s. This rapid signal loss does not reflect the solitonic behavior expected in the ideal KdV, suggesting that the interaction between parameter scaling and discretization led to a numerical collapse. Consequently, the signal fails to preserve a periodic or stable structure, in contrast with the behavior observed in the hyperbolic models.

| Band | Absolute Power | Relative Power |
|---|---|---|
| Alpha | $5.781026 \times 10^{-8}$ | 0.206186 |
| Beta | $3.163888 \times 10^{-8}$ | 0.112858 |
| Delta | $3.335622 \times 10^{-8}$ | 0.118961 |
| Gamma | $1.372356 \times 10^{-7}$ | 0.489035 |
| Theta | $1.478629 \times 10^{-8}$ | 0.072960 |

Tab 5. Absolute and relative power by band (KdV equation, quasilinear dispersive).

The gamma band concentrates nearly 49% of the energy, although with very low absolute values, while the remaining bands exhibit comparable powers without a defined pattern. This outcome reflects more a numerical instability of the simulation than a physically meaningful behavior expected from the Korteweg–de Vries equation.

The associated spectrum confirms the instability of the simulation: absolute powers are on the order of $10^{-8}$, distributed in a highly irregular manner across all bands. No clearly dominant band emerges, and the overall signal energy is extremely low. This indicates that, under the configuration employed, the KdV does not reproduce a coherent response to the musical stimulus and requires parameter adjustment to capture its characteristic dispersive dynamics.

### 4.6 Nonlinear Equation

The following equation was considered:

$$u_t = -\alpha u + \mu (u_{xx})^2 + f(t),$$

in a one-dimensional domain with periodic boundaries. Unlike the previous cases, here the highest-order derivative enters in a nonlinear manner, which characterizes the system as fully nonlinear. The parameter $\alpha$ provides damping, $\mu$ controls the strength of the nonlinearity, and the term $f(t)$ represents the musical stimulus. Integration was performed using centered finite differences and an explicit stable scheme with a time step proportional to $\Delta x^2$.

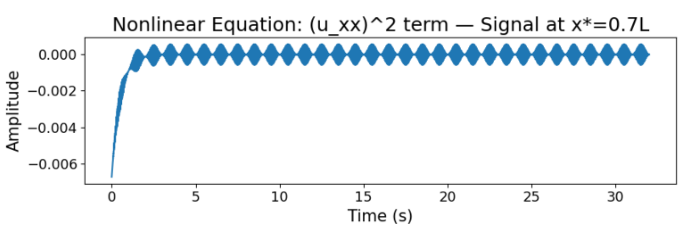


Fig 6. The trace $u(x^*, t)$ at the virtual sensor ($\boldsymbol{x^* = 0.7L}$) exhibited an initial transient phase in which the amplitude increased until stabilizing in a steady oscillatory regime. Unlike Burgers, where energy dissipates rapidly, here the combination of nonlinearity and damping generated a signal that persists over time, with regular periodic oscillations and constant amplitude. Thus, a sustained dynamic is observed, in which the influence of the musical stimulus is preserved in the form of persistent oscillations.

| Band | Absolute Power | Relative Power |
|---|---|---|
| Alpha | $1.979787 \times 10^{-16}$ | $1.834042 \times 10^{-3}$ |
| Beta | $1.435696 \times 10^{-18}$ | $1.330470 \times 10^{-5}$ |
| Delta | $1.588742 \times 10^{-22}$ | $1.471566 \times 10^{-10}$ |
| Gamma | $4.236669 \times 10^{-16}$ | 0.249022 |
| Theta | $1.265504 \times 10^{-15}$ | 0.749630 |

Tab. 6. Absolute and relative power by band (nonlinear equation).

The spectrum shows a clear predominance of the theta band (≈75%), which drives the dynamics with a strong intermediate rhythm. The gamma band (≈25%) acts as a secondary component associated with fast oscillations, while alpha, beta, and delta contribute only marginally. This pattern indicates that, in a fully nonlinear regime, the musical signal is transformed into sustained oscillations dominated by theta with gamma support, in contrast to the strictly linear propagation and the strong dissipation observed in Burgers.

## 5. Conclusions

The study showed that different mathematical formulations lead to contrasting responses to the same musical stimulus. The neuronal activator $\boldsymbol{V(t)}$, modeled as a damped harmonic oscillator, exhibited a sustained response with spectral predominance in the theta band, establishing the physiological reference baseline. The first-order linear equation transmitted the stimulus uniformly without generating new frequencies, thus serving as a comparative baseline. The linear hyperbolic system reproduced the stable coupled propagation of pressure and velocity, with spectral predominance in theta and gamma, reflecting intermediate and fast rhythms in the induced dynamics.

In contrast, the Burgers equation exhibited strong dissipation that eliminated most oscillations, yielding very weak power spectra with no dominant bands, highlighting the attenuating effect of diffusion. The Korteweg–de Vries (KdV) equation failed to sustain a stable pattern under the adopted configuration, showing results dominated by numerical instabilities and very low energies. Finally, the fully nonlinear equation produced a sustained oscillatory regime, with theta as the dominant band and gamma as a secondary contribution, suggesting that nonlinearity can preserve the influence of the stimulus over time.

Taken together, the results highlight that linearity ensures stability but limits spectral complexity, whereas quasilinear and nonlinear formulations introduce additional phenomena such as dispersion, diffusion, or oscillatory persistence. These findings support the value of mathematical modeling as a conceptual framework, paving the way for future work aimed at validating the models with real EEG data and optimizing simulation parameters for applications in computational neuroscience and music therapy.

## *References*


[1] Achermann, P., & Borbély, A. A. (1997). Low-frequency (<1 Hz) oscillations in the human sleep electroencephalogram. *Neuroscience*, 81(1), 213–222. https://doi.org/10.1016/S0306-4522(97)00186-9

[2] Mitchell, D. J., McNaughton, N., Flanagan, D., & Kirk, I. J. (2008). Frontal-midline theta from the perspective of hippocampal "theta". *Progress in Neurobiology*, 86(3), 156–185. https://doi.org/10.1016/j.pneurobio.2008.09.005

[3] Klimesch, W. (1999). EEG alpha and theta oscillations reflect cognitive and memory performance: a review and analysis. *Brain Research Reviews*, 29(2–3), 169–195. https://doi.org/10.1016/S0165-0173(98)00056-3

[4] Engel, A. K., Fries, P., & Singer, W. (2001). Dynamic predictions: Oscillations and synchrony in top–down processing. *Nature Reviews Neuroscience*, 2(10), 704–716. https://doi.org/10.1038/35094565

[5] Jensen, O., Kaiser, J., & Lachaux, J. P. (2007). Human gamma-frequency oscillations associated with attention and memory. *Trends in Neurosciences*, 30(7), 317–324. https://doi.org/10.1016/j.tins.2007.05.001

[6] Koelsch, S. (2010). Towards a neural basis of music-evoked emotions. *Trends in Cognitive Sciences*, 14(3), 131–137. https://doi.org/10.1016/j.tics.2010.01.002

[7] Alluri, V., Toiviainen, P., et al. (2012). Large-scale brain networks emerge from dynamic processing of musical timbre, key and rhythm. *NeuroImage*, 59(4), 3677–3689. https://doi.org/10.1016/j.neuroimage.2011.11.019

[8] Fujioka, T., Trainor, L. J., Large, E. W., & Ross, B. (2009). Beta and gamma rhythms in human auditory cortex during musical beat processing. *Annals of the New York Academy of Sciences*, 1169(1), 89–92. https://doi.org/10.1111/j.1749-6632.2009.04779.x

[9] Lagopoulos, J., Xu, J., Rasmussen, I., et al. (2009). Increased theta and alpha EEG activity during nondirective meditation. *Journal of Alternative and Complementary Medicine*, 15(11), 1187–1192. https://doi.org/10.1089/acm.2009.0113

[10] Calamassi, D., & Pomponi, G. P. (2019). 432 Hz tuned music and the health effect: A double-blind cross-over pilot study. *Explore*, 15(4), 283–290. https://doi.org/10.1016/j.explore.2018.12.005

[11] LeVeque, R. J. (2002). *Finite Volume Methods for Hyperbolic Problems*. Cambridge University Press. https://doi.org/10.1017/CBO9780511791253

[12] Toro, E. F. (2009). *Riemann Solvers and Numerical Methods for Fluid Dynamics*. Springer. https://doi.org/10.1007/b79761

[13] Whitham, G. B. (2011). *Linear and Nonlinear Waves*. Wiley.

[14] Drazin, P. G., & Johnson, R. S. (1989). *Solitons: An Introduction*. Cambridge University Press. https://doi.org/10.1017/CBO9780511624025

[15] Evans, L. C. (2010). *Partial Differential Equations*. American Mathematical Society.

[16] Buzsáki, G., & Draguhn, A. (2004). Neuronal oscillations in cortical networks. *Science*, 304(5679), 1926–1929. https://doi.org/10.1126/science.1099745

[17] Başar, E. (2013). Brain oscillations in neuropsychiatric disease. *Dialogues in Clinical Neuroscience*, 15(3), 291–300. https://doi.org/10.31887/DCNS.2013.15.3/ebasar

[18] Niedermeyer, E., & da Silva, F. L. (2004). *Electroencephalography: Basic Principles, Clinical Applications, and Related Fields*. Lippincott Williams & Wilkins.

[19] Breakspear, M., Heitmann, S., & Daffertshofer, A. (2010). Generative models of cortical oscillations: neurobiological implications of the Kuramoto model. *Frontiers in Human Neuroscience*, 4, 190. https://doi.org/10.3389/fnhum.2010.00190

[20] Jirsa, V. K., & Haken, H. (1996). Field theory of electromagnetic brain activity. *Physical Review Letters*, 77(5), 960–963. https://doi.org/10.1103/PhysRevLett.77.960

[21] Deco, G., Jirsa, V., Robinson, P., Breakspear, M., & Friston, K. (2008). The dynamic brain: From spiking neurons to neural masses and cortical fields. *PLoS Computational Biology*, 4(8), e1000092. https://doi.org/10.1371/journal.pcbi.1000092

[22] Welch, P. (1967). The use of fast Fourier transform for the estimation of power spectra: A method based on time averaging over short, modified periodograms. *IEEE Transactions on Audio and Electroacoustics*, 15(2), 70–73. https://doi.org/10.1109/TAU.1967.1161901

**Contribution of Individual Authors to the Creation of a Scientific Article (Ghostwriting Policy)**
The authors equally contributed in the present research, at all stages from the formulation of the problem to the final findings and solution.

**Sources of Funding for Research Presented in a Scientific Article or Scientific Article Itself**
No funding was received for conducting this study.

**Conflict of Interest**
The authors have no conflicts of interest to declare that are relevant to the content of this article.